

Recent progress in magneto-Archimedes levitation

Yasuhiro Ikezoe

(Department of Applied Chemistry, Nippon Institute of Technology)

<Introduction> Human beings have conducted various experiments using the micro-gravity environment in the space station. For example, if crystals of protein molecules associated with a particular disease can be obtained in space and their structural analysis is successful, we will benefit enormously. Therefore, we are conducting space experiments with a great deal of cost and risk in mind. On the other hand, there are multiple technologies for floating objects on the earth. Magnetic levitation using superconductivity and optical tweezers can be mentioned. However, there are many restrictions such as the need for extremely low temperatures and the fact that only objects of a few microns can be floated. Among them, magnetic levitation is the only technology that can make a macroscopic object stand still in the air in a room temperature environment.

Magnetic levitation is achieved by balancing the repulsive force that a diamagnetic object receives from a magnetic field with the gravity acting on the object. The equation is expressed as follows.

$$B \left(\frac{\partial B}{\partial z} \right) = \frac{\mu_0 \rho g}{\chi} \left\{ \because \left(\frac{\mu_0}{\chi} \right) B \left(\frac{\partial B}{\partial z} \right) = \rho g \right\} \cdot \cdot \cdot (1)$$

Here, χ and ρ is the magnetic susceptibility and density of the substance to be levitated, respectively, and μ_0 is the magnetic permeability of vacuum. The distribution of the magnetic flux density along z-axis is $B(z)$, where the vertical upward direction is defined as the positive direction of the z-axis. The magnetic susceptibility of a diamagnetic object has a negative value, and its absolute value is extremely small, ca 10^{-5} . The magnetic force generated by a magnet is proportional to the magnetic force field, $B(\partial B/\partial z)$. Therefore, a very large magnetic flux density is required to obtain a magnetic force comparable to gravity. Beaugnon et al. demonstrated the magnetic levitation experiment of water for the first time in the world¹⁾, using a huge superconducting magnet that generates a magnetic field of more than 20 T. Even now, such a strong magnetic field is available only in a few institutes in the world. In order to overcome this difficulty, we proposed the principle of magnetic Archimedes²⁾ as a new principle of magnetic levitation. Figure 1 is a schematic diagram showing the principle of Magneto-Archimedes levitation, and the equation for the balance between magnetic force and gravity is expressed as the following equation.

$$B \left(\frac{\partial B}{\partial z} \right) = \frac{\mu_0 \Delta \rho g}{\Delta \chi} \left\{ \because \left(\frac{\mu_0}{\Delta \chi} \right) B \left(\frac{\partial B}{\partial z} \right) = \Delta \rho g \right\} \cdot \cdot \cdot (2)$$

Here, χ_1 and ρ_1 is the magnetic susceptibility and density of the substance to be levitated, respectively. χ_2 and ρ_2 is similarly those of the surrounding medium. $\Delta \chi = (\chi_1 - \chi_2)$ and $\Delta \rho = (\rho_1 - \rho_2)$ is defined as the differences between them. The difference from Eq. (1) is that the density and magnetic susceptibility of the substance to be levitated are regarded as the difference from those of the surroundings. From equation (2), if a paramagnetic object with positive magnetic susceptibility is used as the medium, the magnetic susceptibility difference $\Delta \chi$ can be increased, and the magnetic force field, $B(\partial B/\partial z)$, required for magnetic levitation becomes small. Consequently, magnetic levitation becomes possible with a small magnet. For example, if 10 atm oxygen gas known as paramagnetic gas is used, a magnetic field of about 10 T is sufficient for the levitation of water (Fig. 2). Also, considering the low density of plastics, if a liquid containing paramagnetic ions such as manganese (Mn) or gadolinium (Gd) is used as the medium, magnetic levitation of plastics is realized in the medium using even commercially available permanent magnets. This is because not only increase of $\Delta \chi$ but also decrease of $\Delta \rho$ makes the condition for the magneto-Archimedes levitation much milder. More than 20

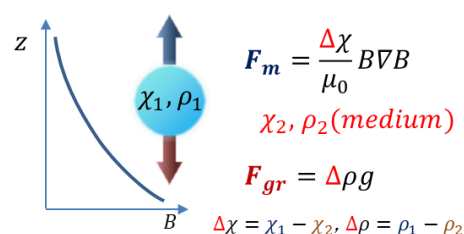


Figure 1. Schematic illustration of principle of magneto-Archimedes levitation



Figure 2. Levitation of water by magneto-Archimedes levitation

years have passed since the magneto-Archimedes levitation was invented, and a large number of applied technologies have been developed. Since then, a few excellent reviews were published.³⁻⁵⁾

[Applications] In a micro-gravity environment inside a space station, an object can be floated but not stationary. This is because there is no minimum point of potential energy of an object in space. The levitation position in the magnetic levitation state is the minimum point of the potential energy of the object. Moreover, since the levitation position is determined by the density and magnetic susceptibility of the object, objects made of different substances levitate in different positions. Taking advantage of this, objects can be separated magnetically in an instant. For example, if a colored glass piece are placed in an aqueous solution of manganese chloride and placed in a magnetic field, the colored glass pieces are instantly separated. If we pour an ethanol solution of manganese chloride between a pair of magnets and put small pieces of polypropylene (PP), polystyrene (PS), or polyethylene terephthalate (PET) in it, these small pieces will fall down due to gravity. However, they are spatially separated due to the repulsive force of the magnets; some can pass between the magnets, however, others cannot (Fig. 3). In recent years, marine microplastics have become a serious problem in the world, but our magnetic separation technology can be considered as a solution for reusing plastics or recovering plastics waste.

The great advantage of levitating an object is that it can remain in non-contact state, however, at the same time it means the object is immobile. We are currently developing a technology to move a levitated object in a non-contact manner using a substance whose magnetism changes by the irradiation of light. For example, the phosphorescent material used for displaying evacuation passages has different valences of Eu ions in the excited state and the ground state, so the magnetism changes depending on whether the light is turned on or off. Therefore, when the phosphorescent material in the magnetic levitation state was repeatedly turned on and off with ultraviolet light, it was found that it moved away from the magnet while it was exposed to light and returned to its original position when the light was extinguished (Fig. 4). This process is reversible, therefore, it is believed that new types of mechanical parts or actuators are realized.

Recently, the performance of computers is so high that it has become easy to simulate the magnetic field distribution in detail. We carried out a precise analysis of the magnetic field distribution near the edges of the permanent magnets, we discovered that when two magnets were placed side by side, water droplets could float in a space of about 1 mm between the two magnets (Fig. 5). This is a great advance in the history of magnetic levitation because, 20 years ago, nobody believed the water is levitated by permanent magnets. In the future, it will be applicable to make a compact surface tension measuring device or liquid supercooling experiments, and so on.

Reference

- 1) E. Beaugnon and R. Tournier, *Nature*, **349**, 470 (1991)
- 2) Y. Ikezoe *et al.*, *Nature*, **393**, 749 (1998)
- 3) S. Ge *et al.*, *Angew. Chem. Int. Ed.* **59**, 17810 (2020)
- 4) J. Xie *et al.*, *Sensor and Actuator B*, **333**, 129533 (2021)
- 5) A. A. Ashkarran and M. Mahmoudi, *Trends in Biotechnology*, **39(3)**, 311 (2021)

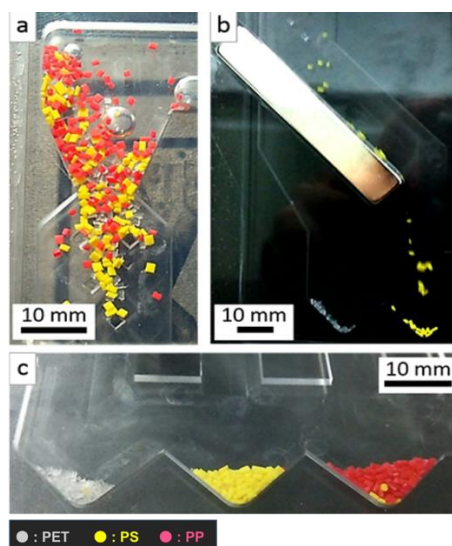


Figure 3. Magnetic separation of plastics pieces, PET, PS and PP. (a) After introducing a mixture of plastics pieces, (b) through a pair of magnet, (c) materials are separated by the magnetic force.

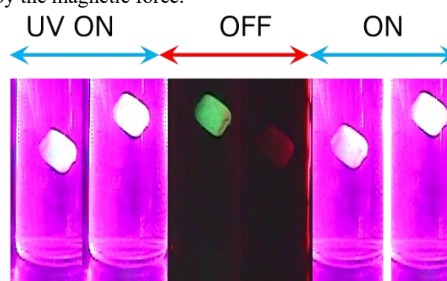


Figure 4. Non-contact manipulation of levitated object by light irradiation. A magnet is located under the bottom of the cell.

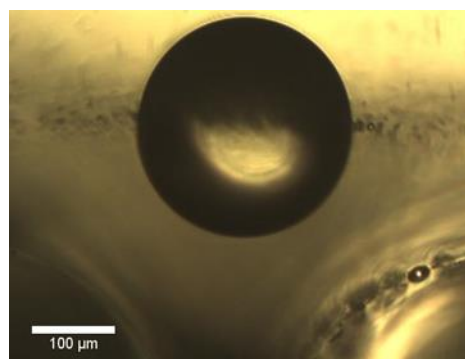


Figure 5. Magnetic levitation of water between two permanent magnets.

Electromagnetophoretic-microfluidic technique for the separation of micro-particles

Yoshinori Iiguni

Nagoya Institute of Technology, Gokiso, Showa, Nagoya 466-8555, Japan

For the detection, separation, and characterization of nm and μm -sized particles, such as biological cells and extracellular vesicles, the method using a microfluidic device is effective, and many researches have been reported. In such the method, the flow pattern design and the transport control of particles in the microchannel are very important techniques. These are governed by introducing a multi-flow, a flow path structure, and applying an external field. In our laboratory, microfluidic analysis of micro-particles based on control of particle transfer in the microchannel utilized electromagnetophoresis with applying the magnetic field and the electric current have been investigated. So far, techniques for separation of micro-particles using the staggered electrophoresis and control of particle transfer based on Lorentz force combined with a conductive/non-conductive aqueous two phase (ATP) micro-flow have been developed.

Separation of micro-particles by Staggered-electromagnetophoresis. When the electric current and the staggered magnetic fields generated by two external magnets are applied to a conductive solution including micro-particles, particles experience two localized electromagnetophoresis (EMP) in a microchannel. As the result, The particles mixture injected from the inlet by the flow of an aqueous medium are once focused near channel wall by EMP force of which direction is orthogonal to the flow. Then, the particles experience the EMP force whose direction is opposite to focusing process. Particles with low EMP migration velocity travel toward the parallel outlet while those with large EMP migration velocity elute off from the diagonal outlet. This elution behavior should result in the separation of the particles based on their sizes or properties. Using this method, we demonstrated the size-based separation of polystyrene (PS) particles (3 and 6 μm in diameter) using localized EMP migration by the magnetic field designed by two Nd-Fe-B magnets. In consequence, both 3 and 6 μm PS particles could be separately recovered at the different outlets with the 100% purity and recovery, respectively. Moreover, yeast cells and 6 μm PS particles could be separated with the high separation efficiency. Currently, application of staggered electromagnetophoresis to plankton analysis is investigated.

Control of particle transfer by electromagnetophoresis combined with ATP micro-flow. When the electric current and the magnetic field are applied to the conductive/non-conductive ATP micro-flow, Lorentz force acts only on the conductive solution (Fig. 2). Therefore, depending on the condition of the ATP flow, electromagnetophoresis of micro-particles only in the conductive fluid and/or convection generated by magnetohydrodynamic (MHD) effect are observed. A double Y-shaped microchip with two inlets, two outlets and a guide on the bottom of the channel was used to form a conductive/non-conductive ATP flow with 1.16 mol L⁻¹ KCl aqueous solution and 20% dextran (Dex) aqueous solution as a conductive fluid and a non-conductive fluid, respectively. PS particles (1, 6 and 10 μm in diameters) and carboxylate PS (cPS) particles dispersed in the conductive fluid could be focused on the ATP flow interface by electromagnetophoresis when Lorentz force was applied to the conductive fluid in the direction opposite to the ATP flow interface. Then, cPS particles were transferred to Dex solution and separated from PS particles. On the other hand, when Lorentz force was applied toward to the ATP flow interface, the rotation of ATP micro-flow by MHD effect was observed in which the positions of the conductive fluid and the non-conductive fluid were interchanged. During the rotation, micro-particles were transferred by both electromagnetophoresis and MHD rotation.

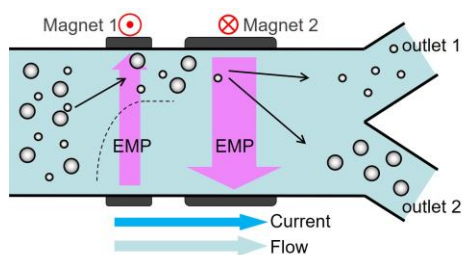


Fig.1 Schematic illustration of staggered Electromagnetophoresis in the microchip

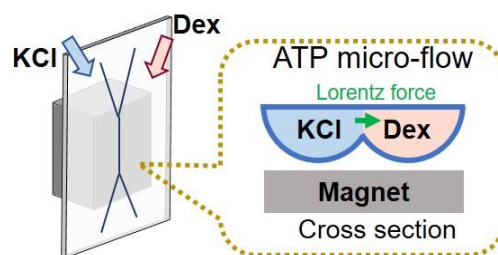


Fig.2 Schematic drawing of Lorentz force acting on the conductive/non-conductive ATP micro-flow

Development of in situ solid-state NMR system for magnetically oriented microcrystal suspensions

Ryosuke Kusumi

Graduate School of Agriculture, Kyoto University, Kyoto 606-8502, Japan

Magnetically Oriented Microcrystal Array (MOMA), i.e., a composite in which microcrystals are aligned three-dimensionally in a polymer matrix by application of a frequency-modulated rotating magnetic field, has a great potential as a means for determination of anisotropic interactions in NMR¹. The 3D orientation of the magnetization axes (χ_1 , χ_2 , χ_3 -axes with $\chi_1 > \chi_2 > \chi_3$), which are related with the crystallographic axes, can be induced by modulated rotation of a microcrystal suspension under a static magnetic field². When such a rotation is performed in an NMR probe, we can determine the anisotropic interactions, e.g., chemical shift tensor, directly from microcrystals in a liquid medium. Recently, we achieved in situ solid-state NMR of a magnetically oriented microcrystal suspension (MOMS) using a probe developed for modulated rotation around an axis perpendicular to the external field³. However, the previous probe only provided one single-crystal (SC) rotation pattern around the χ_3 -axis ($\perp B_0$) of microcrystals. The SC rotation pattern around a general axis, i.e., an axis not perpendicular to B_0 , is required for complete determination of chemical shift tensor.

Here, we developed a new MOMS probe enabling temporal tilt of the axis of modulated-rotation during the period of pulse application and signal acquisition. In this probe (Fig. 1), the microcrystals in the viscous medium are intermittently rotated around the axis normal to the external field (Fig. 1(a)). The magnetization axes of the individual microcrystal are aligned in a reference frame fixed in the modulatory rotating sample, such that the χ_1 -axis is parallel to the initial direction of the external field whereas the χ_3 -axis is to the rotation axis. By temporary tilting the rotation axis (Fig. 1(b)) during the pulse sequence for various rotation angles, SC rotation patterns around an arbitrary axis can be obtained. We successfully measured SC rotation patterns of ¹³C CP spectrum in a MOMS sample of L-alanine in a static magnetic field of 7 T, showing that it is possible to characterize the chemical shift tensor for microcrystals in a liquid medium.

References

- 1) R. Kusumi, F. Kimura, G. Song, T. Kimura, *J. Magn. Reson.* **223**, 68 (2012).
- 2) T. Kimura, F. Kimura, M. Yoshino, *Langmuir* **22**, 3464 (2006).
- 3) R. Kusumi, H. Kadoma, M. Wada, K. Takeda, T. Kimura, *J. Magn. Reson.* **309**, 106618 (2019).

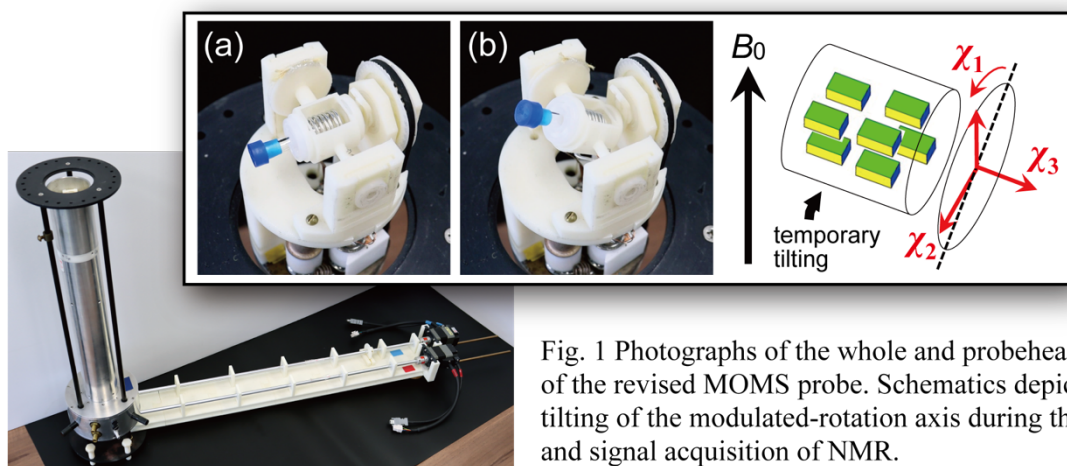


Fig. 1 Photographs of the whole and probehead ((a) and (b)) of the revised MOMS probe. Schematics depicts temporary tilting of the modulated-rotation axis during the pulse application and signal acquisition of NMR.

Magnetic field effect on the preparation process of carbon materials

Atom Hamasaki
(Shinshu University)

Coal tar pitch is a residue left when coal is dry distilled to obtain coke and the like. As it is a residue, even if it is a raw material for activated carbon or graphite now, continuous quest about reuse is important. Coal tar pitch having diamagnetic susceptibility passes through a mesophase, which responds to a magnetic field like a liquid crystal in the heat treatment process. We recently reported that a highly ordered structure of carbonized coal tar pitch due to magnetic orientation was obtained by application of a high magnetic field of 10 T [1]. By using the oriented carbonized material of coal tar pitch as a precursor, the advantages of using magnetic fields in the preparation of activated carbon, graphite, and polarizing elements have been discovered, and I would like to present about these.

【Graphite】 Graphite precursors prepared from coal tar pitch in the absence and presence of a magnetic field of 6 T, which are denoted as general carbonized pitch (GCP) and highly oriented carbonized pitch (HOCP), respectively, were formed into pellets with 20% coal pitch as a binder and then carbonized at more high temperature. The Raman spectra of carbon materials are characterized by a G band around 1600 cm^{-1} derived from the growth of the graphene plane and D band around 1350 cm^{-1} originating from defects in the graphene plane. The dependence of the D-to-G-band intensity ratio (I_D/I_G) of the carbon materials on treatment temperature is plotted in Fig. 1(a) [2]. I_D/I_G of graphite produced from HOCP decreased faster above 1300 K than was the case using GCP. Fig. 1(b) shows the (002) lattice spacing of the carbon hexagonal layer obtained from X-ray diffraction (XRD) measurements. The interplanar spacing of graphite obtained from HOCP is narrower than that from GCP. Therefore, if the precursor is previously oriented, rearranging the crystallites during graphitization becomes relatively easy. As a result, energy was effectively used for crystal growth during the rearrangement process, and graphitization was accelerated.

【Activated carbon】 In order to make activated carbon from pitch, the pitch is generally oxidized near its melting point, which called as stabilization, and then activated. Here, relatively mild environment such as water vapor or carbon dioxide is usually used for activation gas. HOCP (prepared in 10 T) is difficult to be activated because of its highly oriented structure. Therefore, we activated it with potassium hydroxide, which has a high activation ability. The activated carbons prepared from HOCP increased the relative surface area and total pore volume about 30% compared to the that prepared from GCP (prepared in 0 T) as shown in Fig. 2 [3]. Nitrogen adsorption isotherms showed that the pore shapes were almost identical for GCP and HOCP, with more similar holes.

【Polarization property】 Fig.3 shows polarized microscopic images of a prepared thin film (0.15 mm thickness) from coal tar pitch with the absence (a) and presence (b) of 10 T [4]. Those prepared under no magnetic field have domains with a local orientation structure, however, the orientation direction in each was random. Contrastively, those prepared under a magnetic field were completely oriented for the same direction in the range of at least several millimeters. Next, a linearly polarized light was guided to prepare carbon films, and its transmitted light was investigated. Fig. 4 shows the brightness of the transmitted light. In each figure, two kinds of angles formed by the magnetic field axis of the carbonized material and the polarization axis of the linearly polarized light are shown, parallel (open nicols) and orthogonal (crossed nicols). The sample prepared in the magnetic field has functions as a polarizer.

Reference

- [1] Ayumi Sakaguchi, et al. *Chem. Lett.* **2012**, *41*, 1576
- [2] Atom Hamasaki, et al. *AIP Adv.* **2021**, *11*, 025041
- [3] Atom Hamasaki, et al. *Sci. Rep.* **2019**, *9*, 7489
- [4] Atom Hamasaki, et al. *J. Appl. Phys.* **2019**, *125*, 234904

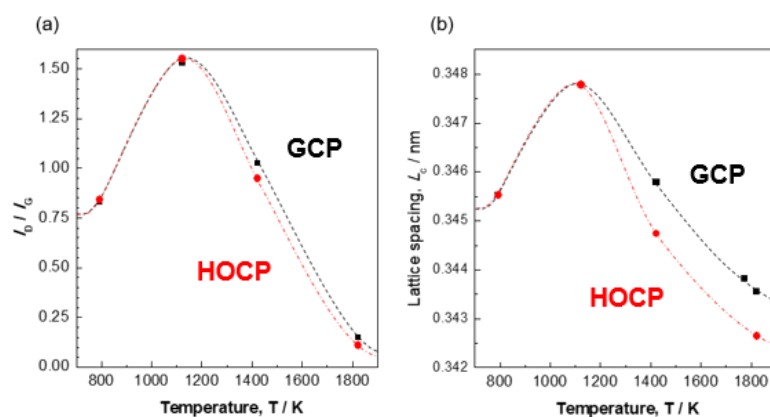


Fig. 1. Heat treatment temperature dependence of (a) the I_D/I_G of Raman scattering spectra and (b) the interlayer spacing of the prepared carbon material from GCP and HOCP.

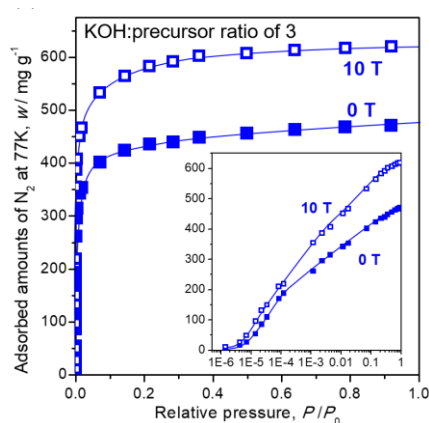


Fig. 2. Adsorption isotherm of activated carbon prepared from GCP (0T, closed marks) and HOCP (6T, open marks). Inset figure is the logarithmic plots.

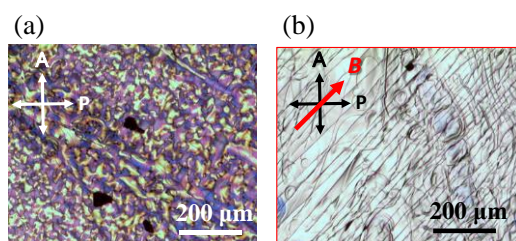


Fig. 3. Polarized microscopic images of a prepared thin film of carbonized coal tar pitch in the absence (a) and presence (b) of a magnetic field and these resistance.

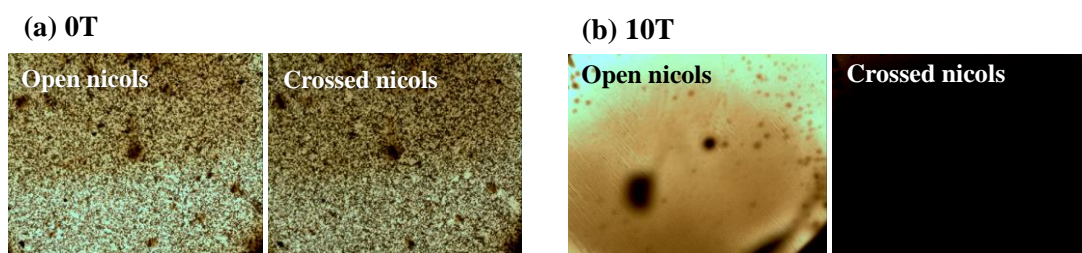


Fig. 4. The brightness of the transmitted linearly polarized light of a carbon thin film prepared in the absence (a) and presence (b) of 10 T at open nicols and crossed nicols positions.

Delay of magnetic field-induced martensitic transformation in some ferrous alloys

Y. Song¹, T. Terai², T. Fukuda², Y. Narumi³, M. Hagiwara³, K. Sato², M. Sugiyama², T. Kakeshita⁴

¹Graduate School of Engineering, Tohoku University, Sendai 980-8579, Japan

²Graduate School of Engineering, Osaka University, Suita 565-0871, Japan

³Center for Advanced High Magnetic Field Science, Osaka University, Toyonaka 560-0043, Japan

⁴Fukui University of Technology, Fukui 910-8505, Japan

Martensitic transformations have been classified into time-independent “athermal transformations” and time-dependent “isothermal transformations” from the viewpoint of kinetics. It had been found that an iron alloy exhibiting an isothermal transformation changes into an athermal transformation by applying pulse magnetic fields¹⁾. This kinetics change has been interesting, and it had been unclear how it changes. The incubation time is particularly interesting because it is related to nucleation, but most of the studies on the incubation time required for martensitic transformation have been about the incubation times longer than one second or more. Therefore, in this study, we aimed to detect an incubation time shorter than one second that cannot be measured with a steady magnetic field, by using a pulsed magnetic field with a large magnetic field sweep rate.

The samples used in this study were Fe-24.8Ni-4.0Mn (at%) and Fe-20.1Ni-5.4Cr (at%) alloys (abbreviate 4.0Mn and 5.4Cr). In both materials, the magnetizations of the martensite phase are larger than those of the parent phase, so a magnetic field can induce martensitic transformation. A rolled plate with a thickness of about 1 mm was prepared by induction melting and hot rolling. From these rolled plates, 4.0Mn was cut out of 5.0 mm × 1.5 mm × 0.30 mm, and 5.4Cr was 5.0 mm × 1.0 mm × 0.30 mm. The 4.0Mn does not have a clear martensitic transformation point even when cooled to 5K at a cooling rate of 2 K / min. However, when it is maintained at an isothermal temperature under a magnetic field of 9 T, it exhibits an isothermal transformation with a nose temperature of around 140 K. The sample was rapidly cooled to 77 K by putting it directly into liquid nitrogen, and then a pulse magnetic field was applied to measure the magnetization. The 5.4Cr has a clear transformation temperature near room temperature and is a sample with remarkable time dependence. The magnetization was measured by applying a pulsed magnetic field to this sample as well.

When a pulse magnetic field with a maximum magnetic field of 25.8T and a pulse width of about 15 ms is applied to the 4.0Mn alloy at 77K, a sharp increase in magnetization due to martensitic transformation is observed at 16.53T. It was. When the same measurement was performed a total of four times, the critical magnetic field varied slightly from sample to sample and ranged from 15 T to 17 T. Next, we conducted an experiment in which a pulsed magnetic field in which the maximum magnetic field was increased by about 0.5 T from around 10 T was applied to the sample until martensitic transformation occurred. Martensitic transformation did not occur when the maximum magnetic field was 13.47 T or less, but when the maximum magnetic field was 14.24 T, a rapid increase in magnetization due to martensitic transformation occurred. However, the transformation occurred 50 μs after the magnetic field reached its maximum value. From this, it can be considered that this transformation requires an incubation period of at least 50 μs. This time is more than enough time for martensite nuclei to grow and is considered to be the time required to form nuclei. In 5.4Cr alloy, the critical magnetic field of martensite transformation depends on the field sweep rate. At 280 K, the value of the critical field was 5.97 T when the sweep rate was 0.015 T / s, while it was 34.01 T for 18.40 × 10³ T / s. These results show there are incubation times much shorter than one second.

Reference

- 1) T. Kakeshita *et al.*, Mater. Trans. JIM, **34** (1993) 415.

Dynamic hysteresis measurement of a magnetic nano particle suspension under a DC bias magnetic field

Reisho Onodera¹, Eiji Kita^{1,2}, and Hideto Yanagihara²
(NIT, Ibaraki college¹, Univ. of Tsukuba²)

Introduction

Magnetic nanoparticles (MNPs) have already been utilized as contrast agents in MRI and are also being investigated for applications in magnetic hyperthermia, magnetic nanoparticle imaging (MPI), and a drug delivery system. Magnetic hyperthermia uses the heat generated in MNPs by applying an alternating magnetic field (AMF), and the heating ability of MNPs depends on the energy loss in the dynamic hysteresis loop, therefore the dynamic magnetization curve obtained by applying AMF has been studied experimentally and theoretically.

In MPI, two types of magnetic fields are used for a direct current field (DC-MF), which creates a zero-field region, and an AMF, which induces the magnetization of MNPs in the zero-field region. In addition, magnetic hyperthermia has been investigated in combination with the drug delivery system using DC-MF to concentrate and retain MNPs in the affected part.

Thus, it is important to evaluate the magnetic properties of MNPs under the condition that DC-MF is combined with AMF, because DC-MF and AMF are expected to be used together in many medical applications of MNPs.

In this study, we have investigated the dynamic hysteresis of Resovist[®], a commercial superparamagnetic iron oxide when parallel and perpendicular DC-MFs are applied to the AMF, in order to evaluate the effect of DC-MFs on the high-frequency responsiveness of a magnetization.

Experimental setup

The system consists of a DC-MF magnet and an AC magnetization measurement system¹⁾. As shown in Fig. 1, an electromagnet with 50 mm diameter poles is used for DC-MF generation, and AMF generation coils for dynamic hysteresis measurement and magnetization and magnetic field detection coils are installed between the poles. The AMF generator consists of a series LC resonant circuit consisting of an air-core coil and a capacitor, and a high-frequency power supply (1 kW), which can generate a high-frequency magnetic field in the range of 20 k to 1 MHz. The magnetic poles of the DC-MF, the AMF coil, and the detection coil are arranged as shown in Fig. 1, and the applied direction of the DC-MF can be changed between parallel and perpendicular.

Experimental results

Dynamic hysteresis measurements were carried out with the DC field strength and AC field amplitude of 0-50 mT and 5-70 mT, respectively, and the frequency range of 60-200 kHz.

As a result of the measurement, the hysteresis loop of the applied DC-MF perpendicular to the AMF showed linear response with increasing DC-MF strength, while the coercivity in the dynamic loop did not change significantly.

When parallel DC-MF was applied, the slope of the loop showing linearity changed with the intensity of DC-MF in the small range of AMF amplitude. In this talk, we will introduce the effect of the DC field by comparing the results with static magnetization measurements by using a VSM.

Reference

- 1) A. Seki, *et al.*, J. Phys.: Conf. Ser., **521** (2014) 012014.
- 2) R. Onodera, *et al.*, IEEE Trans. Mag., **57** 6100605 (2021).

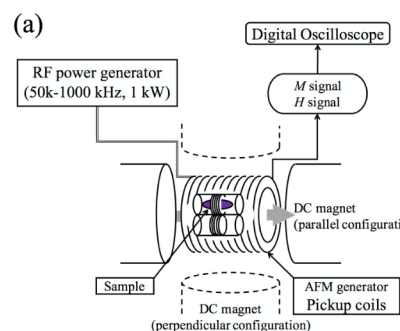


Fig. 1 Schematic diagram of the experimental setup. ²⁾

In-field annealing for precipitation of magnetic alloys

Y. Mitsui¹, M. Onoue², S. Kuzuhara³, W. Ito³, and K. Koyama^{1,2}

¹ Graduate School of Science and Engineering, Kagoshima University, Kagoshima 890-0065, Japan

² Research Support Center, Institute for Research Promotion, Kagoshima University, Kagoshima 890-0065, Japan

³ National Institute of Technology, Sendai College, Natori 981-1239, Japan

Magnetic field effects on the phase diagram, phase transformation, microstructures, and diffusion of the magnetic alloys have been studied so far. Phase transformation or reaction to the ferromagnetic phase were enhanced by application of magnetic fields, while those to non-ferromagnetic phase from ferromagnetic phase were suppressed under magnetic fields^{1,2)}, because the energy gain of magnetic phase under magnetic fields depends on magnetic field intensity and magnetization of the phase. Furthermore, when phase diagram is changed by magnetic field, phase fraction of the equilibrium phases can be controlled.

On the other hand, magnetic field has been used for separation of the magnetic particles and the non-magnetic ones³⁾. In the viewpoint of gain of magnetic energy, magnetic-field-induced precipitation can be expected by difference of magnetization of the phases. In other words, novel magnetic separation method by in-field annealing can be expected.

In this study, we report the magnetic field effects on the precipitation of ferromagnetic and non-ferromagnetic elements. We focused on the magnetic field effects on the precipitation of non-magnetic elements Cu in iron and that of iron due to the decomposition of rare-earth permanent magnet $\text{Sm}_2\text{Fe}_{17}\text{N}_3$. The phase fraction and precipitation behavior was evaluated by ^{57}Fe Mössbauer spectroscopy.

Table 1 shows the phase fraction of the Sm-Fe-N annealed in 0 and 5 T. $\text{Sm}_2\text{Fe}_{17}\text{N}_3$ decomposed into Sm_2O_3 and αFe , iron-oxide compounds due to the oxidation and the existence of Fe_2O_3 . After in-field annealing at 5 T, phase fraction of Fe-based phase become larger than those at 0 T. Therefore, it is found that decomposition of Sm-Fe-N phase and the precipitation of Fe and Sm_2O_3 was enhanced by in-field annealing.

In the presentation, magnetic field effects on Fe-Cu and $\text{Sm}_2\text{Fe}_{17}\text{N}_3$ systems are discussed in the viewpoint of magnetic properties of the phases at the reaction and the phase diagram in magnetic fields.

Table 1. Phase fraction of Sm-Fe-N phase and Fe-based phase

	Phase fraction of Sm-Fe-N ($\text{Sm}_2\text{Fe}_{17}\text{N}_3$ + $\text{Sm}_2\text{Fe}_{17}\text{N}_x$ phase (%)	Phase fraction of Fe-based (αFe + Fe_2O_3 + Fe_3O_4) phase (%)
0 T	85.3	14.7
5 T	65	35

Reference

- 1) Y. Mitsui *et al.*, J. Alloy. Compd., **615** (2014) 131-134.
- 2) R. Kobayashi, *et al.*, Mater. Trans. **58** (2017) 1511-1518.
- 3) N. Hirota *et al.*, J. Magn. Magn. Mater. **427** (2017) 296-299.